

Finding the best thickness run parameterization for optimization of Tailor Rolled Blanks

Niklas Klinke¹, Axel Schumacher²

¹ Mubea Tailor Rolled Blanks GmbH, TRB Product Development, P.O. Box 472, D-57428 Attendorn, Germany, niklas.klinke@mubea.com, +49 (0)2722 62 6170

² University of Wuppertal, Faculty 7, Chair for optimization of mechanical structures, Gaußstraße 20, D-42119 Wuppertal, Germany, schumacher@uni-wuppertal.de, +49 (0)202 439 2386

1 Introduction

Typical Body in White (BiW) parts are subjected to numerous loadcases from different disciplines (Crash, NVH, and Durability). In combination with several design boundaries like design spaces, manufacturability and cost, the resulting parts mostly show inhomogeneous material utilization. Together with the interest in reducing CO₂ emissions by saving weight in structural parts tailored blank technologies help to increase material utilization and therefore reducing part masses [1].

Tailor Rolled Blanks (TRB) are an established lightweight application for highly stressed structural parts in automotive industry. By varying the rolling gap, parts with load adapted thickness profiles and continuous transitions are manufactured (Fig.1). Typical benefits of using TRB are weight reduction, part integration or fine tuning of performance. Different to other tailored blank technologies the number of different thicknesses in a part does not drive the part cost. Compared to Tailor Welded Blanks (TWB) the stress distribution in transition areas doesn't show any inconstancy due to the sudden increase in thickness. Also it was shown that TRB has good forming characteristics because of the removal of the weld seam and the heat affected zone [2]. The rolling process itself is subjected to several manufacturing constraints like the maximal thickness reduction or the maximal slope which have to be taken into account in the design optimization.

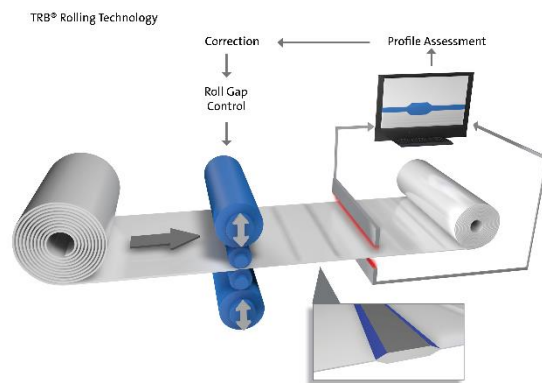


Fig.1: Flexible Rolling

In order to design the thickness run and efficiently find lightweight potentials optimization techniques are used. The publications [3] and [4] show the potential of TRB for BiW application by using optimization techniques. Different parametrization approaches were used to control the part thickness distribution. The question arising here is: What is the best thickness run parameterization for a given problem? Therefore, we compare different parametrization approaches.

The optimization problem is formulated for the use in typical automotive development processes. LS-OPT is used for metamodel-based optimization of a hotformed sheet metal profile subjected to different dynamic bending loadcases. Radial Basis Functions (RBF) are used as metamodels in conjunction with adaptive simulated annealing (ASA) as optimization algorithm. Results are compared on behalf of performance, mass and function calls. As a result we present recommendations for the best thickness run parametrization.

2 Design of TRB Parts

2.1 Manual design of TRB Parts

As stated above many conventional BiW parts are stressed inhomogeneously. By reviewing the deformation kinematic or the distribution of internal energy a CAE Engineer is able to create a TRB part by intuition and engineering judgement. Fig.2 shows a typical TRB B-Pillar. Since a B-Pillar has to fulfill numerous functional requirements the design of the thickness run is highly complex and takes various iterations in different loadcases. In an increasingly fast and complex design environment sophisticated design methods are necessary.

2.2 Design by optimization

The field of numerical optimization offers a wide range of techniques and algorithms which help to design or improve systems. On the field of automotive body optimization the number of algorithms used is limited because of the high computational effort and the non-linearity in of crash analysis. Mainly two groups of techniques are used which are metamodel based methods and global search algorithms (Genetic algorithm (GA), Simulated Annealing (SA), Differential Evolution (DE)).

Global search strategies need a high number of function calls but are likely to leave local optima behind.

Metamodel based strategies build a response surface based on a random sampling of the design space. Optimization with global search algorithms is then carried out on the metamodel. Since the metamodel is a mathematical representation of a system even a huge number of function calls in the global optimizer routines are neglectable when compared to the runtime of the crash analysis. [5,6]

The outcome of metamodel based optimization is depending on the metamodel quality which can be assessed with statistical measures. Due to several advantages like exchangeability among different departments, fast evaluation of different scenarios, utilization in robustness assessment, metamodel based optimization techniques have become a standard technique of multidisciplinary optimization (MDO) workflows.

2.3 State of the art in parametrization of TRB

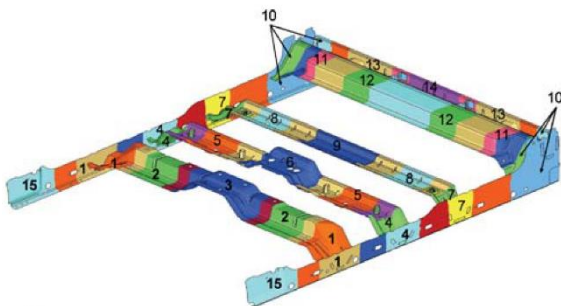


Fig.3: Parametrization with fixed plateau boundaries (FPB) [3]



Fig.2: Mubea B-Pillar with colored thickness run. Light grey: Thin plateau. Dark grey: Thick plateau. Blue: Thickness transition

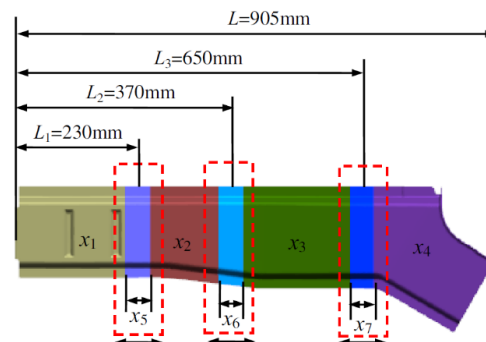


Fig.4: Parametrization with moving plateau boundaries (MPB) [4]

It has been shown in [3] that with the aid of metamodel based optimization it is possible to design TRB parts in an industrial MDO process. Six parts of a truck underbody were parameterized by dividing the parts in several properties as shown in Fig.3. Thickness transition zones were defined by setting their thickness to the mean of their adjacent thicknesses. The parameterization is a fixed plateau boundaries (FPB) parametrization, because the plateaus cannot be moved. Design constraints were imposed on maximum thickness difference between two adjacent plateaus (maximum slope of $0.01 \frac{mm}{mm} - 1 mm$ thickness change per $100 mm$ rolling length) and on maximum thickness reduction per part (maximum rolling reduction of 50 %). The optimized underbody design met the functional requirement and achieved weight saving.

In [4] the inner front longitudinal beam of a vehicle was replaced with an optimized TRB part. A four plateau parametrization was used with additional design variables on the middle point of the transition zones as well as their width (Fig.4). This parametrization has movable plateau boundaries (MPB). Constraints on the design variables were imposed on the minimal slope length ($40 mm$) and the maximum slope ($0.01 \frac{mm}{mm}$). The maximum thickness reduction (50 %) was constraint by the selection of the variable bounds. For the part a mass reduction of 15 % was achieved while also improving the crashworthiness by influencing the folding behavior in a positive way.

3 Strategy for finding the best thickness run parametrization

Since the parametrizations used in literature can roughly be separated in those with fixed plateau boundaries (FPB) and moving plateau boundaries (MPB), we want to compare those with different number of plateaus. Both parametrizations have different dependency on the number of thickness variables, thus only parametrization with the same number of design variables (4, 7 and 10) are compared.

A sequential metamodel-based optimization scheme is used in conjunction with a reduction of the sampling domain (SRSM). $1.5(n + 1) + 1$ design points are added sequentially in each iteration by a space filling sampling. Since the location of the sampling points is depending on a random number generator, the metamodels might be significantly different in early iterations. The SRSM subdomain is depending on the predicted optimum on the specific metamodel. Hence the whole optimization progress is strongly depending on the random number seed.

To reduce the influence of the random sampling on the results, it would be possible to use more sampling points at each iteration. This would lead to better metamodel quality and therefore to less influence of the random seed. In an industrial optimization process the number of designs, resp. function calls, which need to be evaluated to reach an optimum is important because it determines the turnaround time for optimization studies. We therefore used a minimal number of points for each iteration. For all studies shown in this paper, we carried out 10 independent optimization runs with different seeding values and therefore different sets of the space filling samples. The result is a distribution of the optimal values depending on these different sets. So, based the 10 optimizations, we get the expectation value μ and the variance σ and have an idea, how robust the optimization using few function calls is. With this study, we are able to identify the best parametrization analyzing the statistical scatter of the optimal results.

3.1 TRB Modelling

At Mubea transition zones are realized by applying linear interpolated nodal thicknesses. In-house software applies a thickness run to an existing FE-Mesh without changing the Mesh itself. This approach is more precise since the transitions are modeled as fine as possible. Also no remeshing or update of connection entities is necessary, which makes pure thickness optimization process more stable.

3.2 FPB Parametrization

The first parametrization we want to use is comparable to the parametrization in [3] because the plateaus cannot be moved. Different to [3] the part is divided into several equally large strips.

For every additional plateau one design variable is added. The variable bounds are listed in Table 1. Here n is the number of plateaus.

In order to ensure rollability of the thickness profile up to a certain point the constraints listed in Table 2 are applied. It can be seen that the variable boundaries are linked implicitly through the design constraints. For TRB steel parts red_{max} is typically 50 %. The maximum slope s_{max} is 0.01 (1 mm thickness change per 100 mm rolling length). Here l_{TZ} is the length of the particular transition zone.

Table 1: Variable bounds on FPB parametrization

Name	Lower bound	Upper bound
$t_i, i \in \{1, \dots, n\}$	t_{min}	t_{max}

Table 2: Design constraints on FPB parametrization

Name	Number of Constraints	Expression	Constraint
Thickness reduction	1	$1 - \frac{\min(t_i)}{\max(t_i)}$	$\leq red_{max}$
Slope $_{i,i+1}$	$n - 1$	$\frac{ t_i - t_{i+1} }{l_{TZ}}$	$\leq s_{max}$

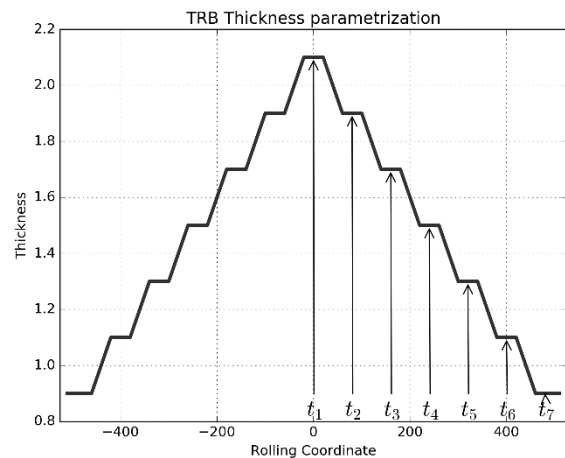


Fig.5: Fixed plateau boundaries (FPB) parametrization with 7 design variables (7 thicknesses)

3.3 MPB Parametrization

The second parametrization is closer to [4] because the plateau boundaries are able to be moved along the profile. The design bounds of this parametrization are set very wide to not include any knowledge.

For every additional plateau which should be movable three new design variables are added (two position variables, one thickness). The bounds of the design variables can be reviewed in Table 3. Beginning and end position ($x_{1,B}$ and $x_{n,E}$) have to be set according to the part dimensions. For the other position variables the bounds can be derived based on a minimum length of plateau $l_{p,min}$ and transition $l_{TZ,min}$ and chain dimensioning.

In Table 4 the design constraints are listed. The thickness reduction constraint is comparable to FPB. For the slope constraint the complexity is increased because the fraction denominator is not constant anymore. MPB parametrizations has $2(n - 1) + n$ more constraints compared to FPB.

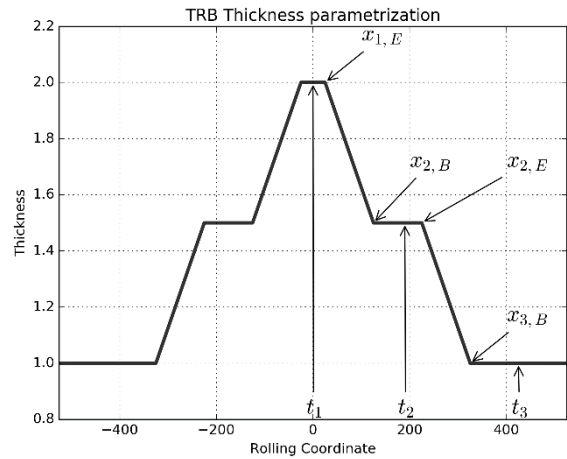


Fig.6: Moving plateau boundaries (MPB) parametrization with 7 design variables (3 thicknesses and 4 positions)

Table 3: Variable bounds on MPB parametrization

Name	Lower bound	Upper bound
$t_i, i \in \{1, \dots, n\}$	t_{min}	t_{max}
$x_{1,B}$	Beginning point of part or symmetry line	
$x_{i,E}, i \in \{1, \dots, n\}$	$x_{i,B} + l_{p,min}$	$x_{i+1,B} - l_{TZ,min}$
$x_{i,B}, i \in \{2, \dots, n\}$	$x_{i-1,E} + l_{TZ,min}$	$x_{i-1,E} - l_{p,min}$
$x_{n,E}$	Endpoint of part	

Table 4: Design constraint on MPB parametrization

Name	Number of constraints	Expression	Constraint
Thickness reduction	1	$1 - \frac{\min_i(t_i)}{\max_i(t_i)}$	$\leq red_{max}$
Plateau _i	n	$x_{i,E} - x_{i,B}$	$\geq l_{p,min}$
Slope _{i,i+1}	$n - 1$	$\frac{ t_i - t_{i+1} }{x_{i+1,B} - x_{i,E}}$	$\leq s_{max}$
Slope length _{i,i+1}	$n - 1$	$x_{i+1,B} - x_{i,E}$	$\geq l_{TZ,min}$
thickness difference _{i,i+1}	$n - 1$	$ t_i - t_{i+1} $	$\geq \Delta t_{min}$

4 Application Example

4.1 Part and Loadcases

We use a hot formed w-profile of $1000 \times 165 \times 35 \text{ mm}$ dimensions subjected to a dynamic three point bending loadcases. A cylindrical rigid impactor with 150 mm diameter, weighting 180 kg is impacting with $20 \frac{\text{km}}{\text{h}}$ in the middle of the profile. At the ends the part is laying on two cylindrical rigid walls. Gravity is applied to the whole model. Coulomb friction was used with friction coefficient of 0.1. A strain rate dependent elasto-plastic material was used to describe the material behavior of the profile. No fracture model was included.

As a first loadcase (X000) the impactor is placed at $x = 0 \text{ mm}$. In order to generate more complex thickness runs a second loadcase (X200) is added with a impactor located at $x = 200 \text{ mm}$. The thickness run of this profile is set to be symmetric to $x = 0 \text{ mm}$. Fig.7 shows the first loadcase (X000) and the symmetry plane.

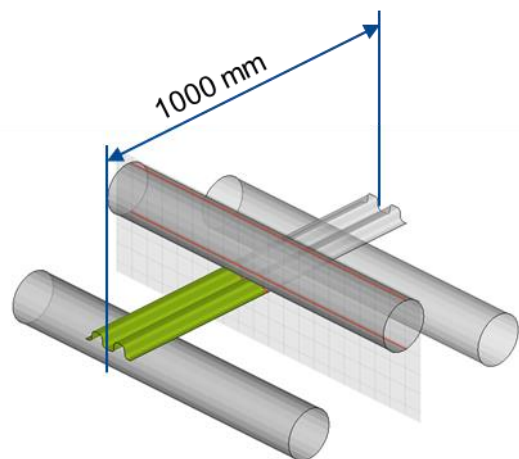


Fig.7: Loadcase with impactor at $x = 0 \text{ mm}$ in undeformed condition with a symmetry plane for the thickness run at $x = 0 \text{ mm}$

As a baseline the profile is crashed with 2 mm constant thickness. In this configuration the part weight is 3.750 kg. The functional constraint is then derived from the maximum impactor displacement. For the 2 mm profile the maximum displacement is at approximately 100 mm. In Fig.8 and Fig.9 the loadcases X000 and X200 are shown at maximum deformation.

The two loadcases are used to build up two optimizations with different loadcase setups. Loadcase setup A is only using loadcase X000, while loadcase setup B is using both loadcases X000 and X200. Since loadcase setup B has two impactors we expect a more complex thickness run.

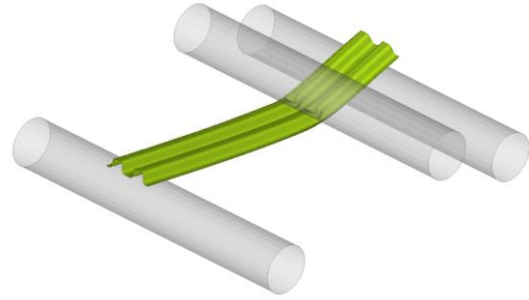
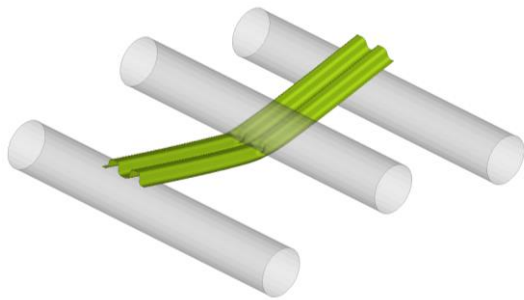


Fig.8: Maximum deformation for baseline profile and loadcase X000

Fig.9: Maximum deformation for baseline profile and loadcase X200

4.2 Optimization Setup

LS-OPT is used for metamodel based optimization. The optimization problem can be formulated as follows: $\min mass$, $d_i \leq 100\text{ mm}$, where d_i is the maximum displacement of the corresponding impactor. The optimization flowchart for loadcase setup B can be reviewed in Fig.9. The Setup is containing the design variables and their design boundaries. In the sampling stage $1.5(n + 1) + 1$ design points are generated by a space filling sampling. These designs are then calculated in the loadcases X000 and X200 (described in 4.1). Afterwards the stages X000R and X200R extract the results. When the results of all designs in an iteration are extracted, a radial basis function (RBF) metamodel is built upon the responses. The optimization stage is then performing a hybrid optimization with adaptive simulated annealing (ASA) as a global optimizer and the leapfrog (LF) algorithm for local. Afterwards the predicted optimum is compared with the last predicted optimum (or the baseline design) to check if the termination criteria is met. If the design and objective change is below 1 % the optimization process is converged and the latest predicted optimum is verified in an additional single design iteration. If the termination criteria is not met the sampling domain is reduced by the SRSM scheme in direction of the predicted optimum and a new sampling is generated. The maximum number of iterations is set to 20. If this number is reached the latest predicted optimum is verified and the optimization is terminated without convergence.

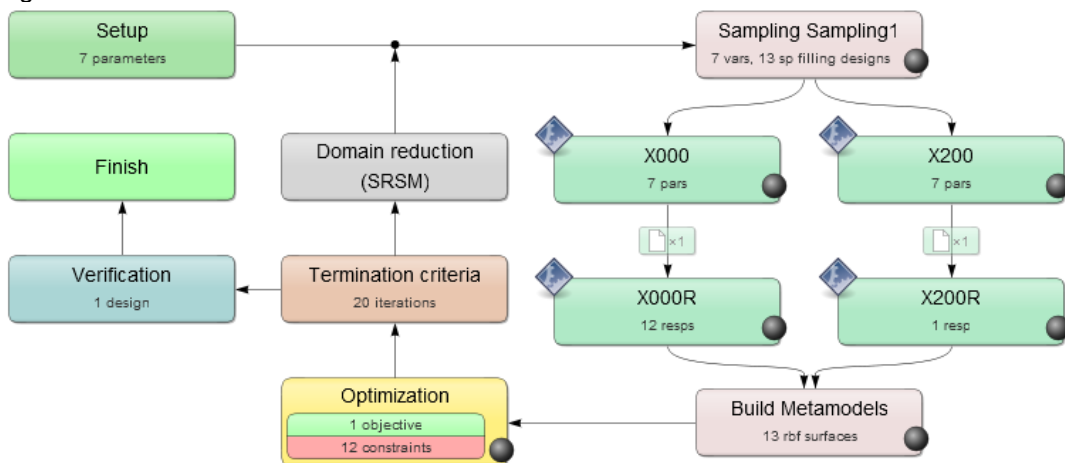


Fig.9: LS-OPT optimization flowchart for loadcase setup B. For loadcase setup A, X200 and X200R are missing.

5 Results

The following figures and tables present the results of the optimization studies for both loadcase setups. In the left plot the baseline design (black horizontal line) and the optimal thickness run of each optimization is shown. Maximum constraint violation of the latest optimum is used to judge the quality of the optimized design. The scatter of the design quality can be reviewed in the middle plot. In the right plot the distribution of the number of design points can be reviewed which represents the numerical effort. Also the maximum number of designs for the specific number of design variables (dv) is shown as a horizontal red datum line.

Table 5 and Table 6 show the expectation value μ and the variance σ for the different sets of optimizations. The scatter in the number of evaluated designs leads to odd numbers in the mean column for the number of designs.

5.1 Loadcase Setup A

In Fig.10 the results are shown for loadcase setup A grouped by optimization with the same number of design variables. Fig.11 shows all optimization results for the design quality and the numerical effort, only the thickness run plot is limited to one representative thickness run.

All optimal thickness distributions upgauge the impact area at $x = 0$ mm by 0.2 – 0.4 mm while reducing the thickness in the bearing areas by 0.8 – 0.9 mm. The overall tendency of the thickness runs is quite comparable.

For the 7 thickness and 10 thickness FPB parametrizations it can be seen that the minimal thickness is higher compared to the other optima. This might be due to the thickness reduction constraint, which limits the minimum thickness to half the maximum thickness.

When comparing the design quality in Fig.10 the MPB parametrizations show higher mass savings than the FPB parametrizations. In terms of max. constraint violation the scatter of results is comparable for the same number of design variables.

The number of design points for the FPB parametrizations is low compared to the MPB ones. More than half of the MPB parametrizations reached their maximum number of iterations, while none of the FPB parametrization does.

To compare the results a statistical summary is listed in Table 5. When comparing the mean objectives the MPB parametrizations have 0.6 – 1.1 % higher weight savings, where 1 % means 0.0375 kg. Looking at the mean number of design points the MPB parametrizations use more than three times the number of function calls.

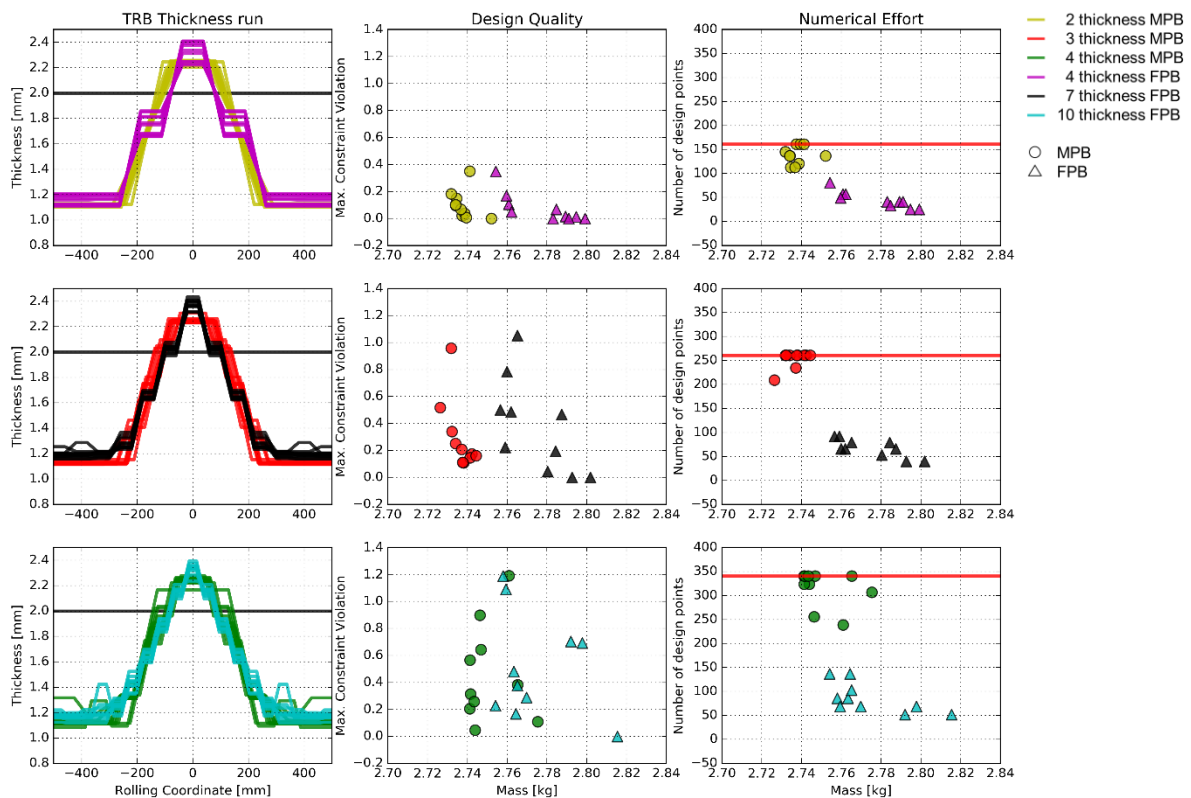


Fig.10: Results for loadcase setup A, grouped by number of design variables

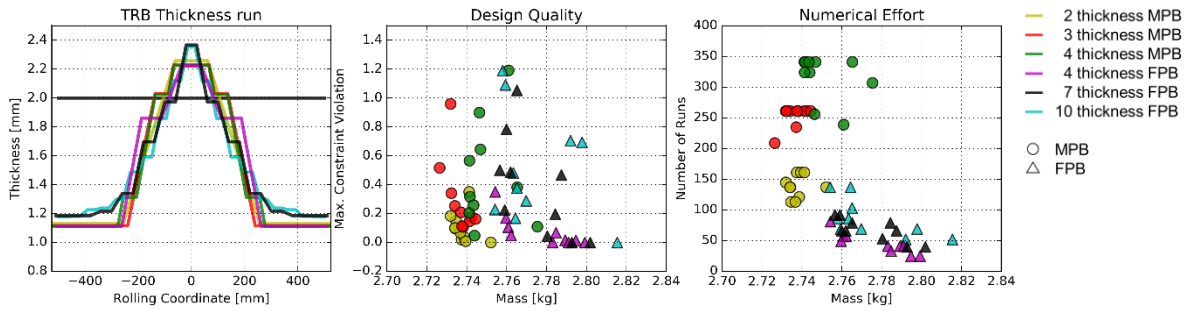


Fig. 11: All results for loadcase setup A with representative thickness run

Table 5: Result summary of loadcase setup A

	dv = 4				dv = 7				dv = 10			
	MPB		FPB		MPB		FPB		MPB		FPB	
	μ	σ	μ	σ	μ	σ	μ	σ	μ	σ	μ	σ
Iterations	18.20	2.35	6.50	2.12	20.40	1.35	6.10	1.45	19.50	2.22	6.00	1.83
Constraint Vio.	0.10	0.11	0.08	0.11	0.30	0.26	0.38	0.35	0.46	0.37	0.52	0.39
Objective [kg]	2.738	0.008	2.779	0.015	2.738	0.004	2.775	0.015	2.753	0.011	2.775	0.019
Runs	138.60	18.78	45.00	16.97	253.20	17.55	67.30	18.84	315.50	37.80	86.00	31.04

5.2 Loadcase Setup B

In Fig.12 the results are shown for loadcase setup B grouped by optimization with the same number of design variables. Fig.13 shows all optimization results for the design quality and the numerical effort, only the thickness run plot is limited to one representative thickness run.

The weight saving achieved by the MPB parametrizations is again higher compared to those of the FPB optimizations. Only for the MPB parametrization with two thicknesses the mean objective value is 0.5 % worse than the corresponding FPB mean objective. This is due to the fact that the 2 thicknesses cannot adapt to the two impactor positions efficiently. The mean number of design points used by the MPB parametrizations is approximately two times as high as for the FPB, where the mean number of design points used by MPB optimizations are comparable to loadcase setup (A) but the mean number of points used by FPB optimization nearly doubled.

Table 6: Result summary of loadcase setup B

	dv = 4				dv = 7				dv = 10			
	MPB		FPB		MPB		FPB		MPB		FPB	
	μ	σ	μ	σ	μ	σ	μ	σ	μ	σ	μ	σ
Iterations	13.50	4.28	8.00	1.33	20.20	1.75	10.00	4.83	18.70	3.68	10.00	4.35
Constraint Vio.	0.09	0.15	0.44	1.06	0.29	0.30	0.30	0.44	1.12	2.85	0.64	0.95
Objective [kg]	2.981	0.019	2.963	0.011	2.918	0.008	2.925	0.008	2.918	0.008	2.933	0.030
Runs	101.00	34.20	57.00	10.67	250.60	22.77	118.00	62.80	301.90	62.62	155.60	74.06

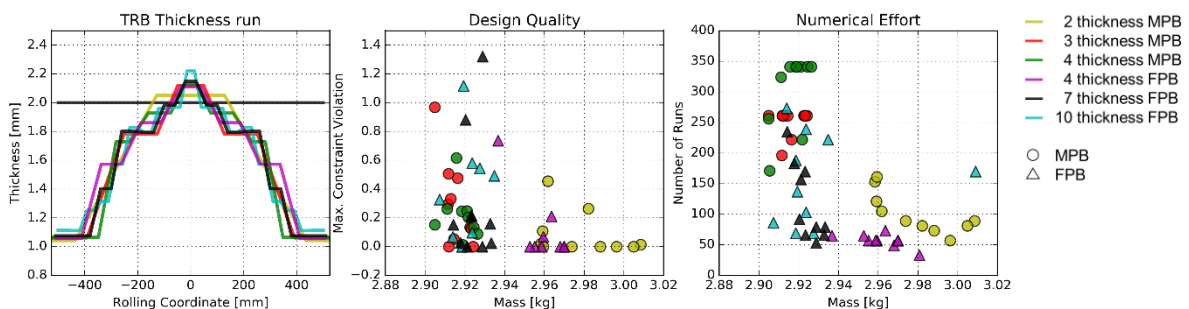


Fig. 13: All results for loadcase setup B with representative thickness run

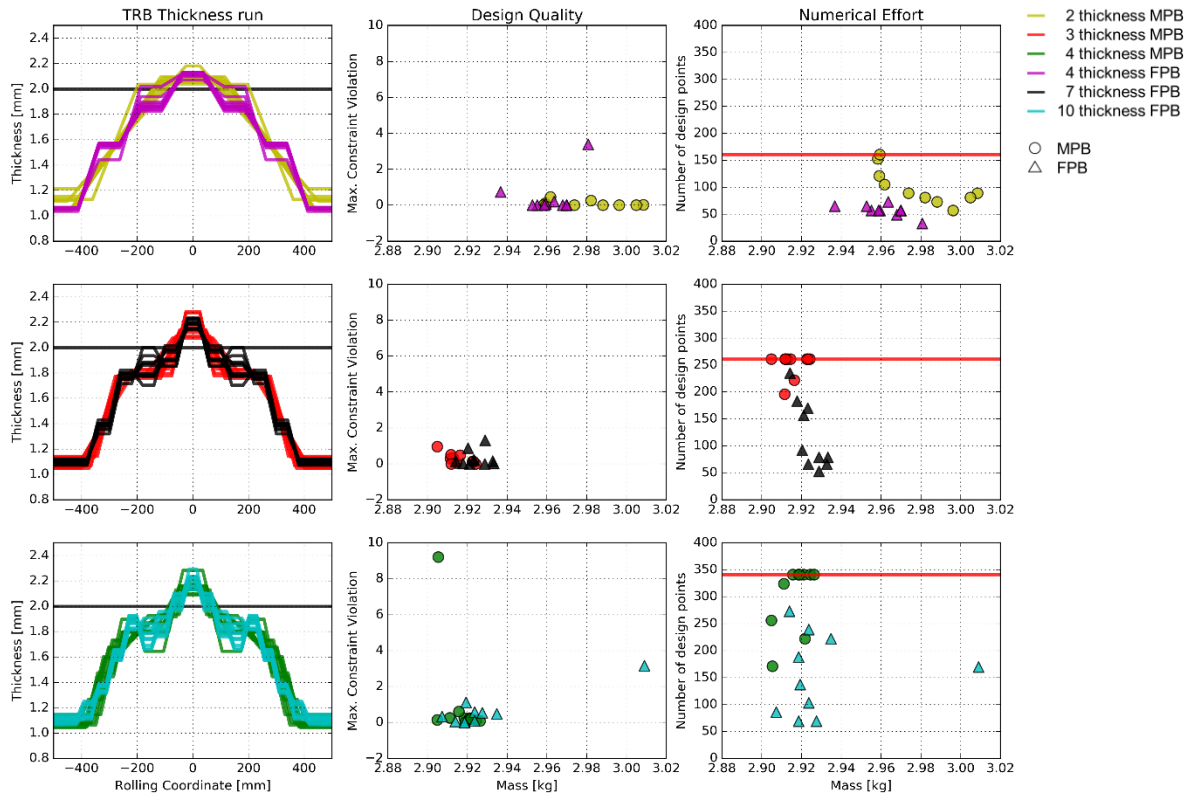


Fig. 13 Results for loadcase setup B, grouped by number of design variables

6 Summary

It could be shown that the choice of the thickness run parametrization has a significant influence on the total number of runs used to reach a converged optimum. Nevertheless the resulting thickness runs are roughly comparable in shape. MPB parametrizations show a higher mass reduction. For loadcase setup (A) engineering judgement tells us that a good thickness run probably is a symmetric two plateau design. Hence the results show that the MPB parametrization is effective if the number of plateaus is adjusted to the right value a priori (2 thickness MPB for loadcase setup A). MPB parametrization with a higher number of plateaus did not lead to better results here. If the number of plateaus in a part cannot be derived from engineering knowledge, for example in loadcase setup (B), the usage of a high number of movable plateaus (MPB) proved to be inefficient compared to the corresponding FPB parametrizations.

Our proposal is therefore to use MPB parametrization in cases where the number of plateaus is already known and to use FPB parametrization otherwise.

7 Literature

- [1] M. Merklein, M. Lechner, Manufacturing Flexibilisation of Metal Forming Components by Tailored Blanks, 2013.
- [2] R. Kopp, C. Wiedner, A. Meyer, Flexible rolling for load adapted blank, International Sheet Metal Review, (4) (2005) 20–24.
- [3] C.H. Chuang, R.J. Yang, G. Li, K. Mallela, P. Pothuraju, Multidisciplinary design optimization on vehicle tailor rolled blank design, Struct Multidisc Optim 35 (6) (2007) 551–560.
- [4] L. Duan, G. Sun, J. Cui, T. Chen, A. Cheng, G. Li, Crashworthiness design of vehicle structure with tailor rolled blank, Struct Multidisc Optim 53 (2) (2016) 321–338.
- [5] N. Stander, W. Roux, A. Basudhar, Eggleston Trent, T. Goel, K. Craig, LS-OPT® User's Manual: A DESIGN OPTIMIZATION AND PROBABILISTIC ANALYSIS TOOL FOR THE ENGINEERING ANALYST. Version 5.2, 2015.
- [6] A. Schumacher, Optimierung mechanischer Strukturen: Grundlagen und industrielle Anwendungen, 2nd ed., Springer Vieweg, Berlin, Heidelberg, 2013.